Landmarks in Earth Reinforcement, Ochiai et al. (eds),
© 2001 Swets & Zeitlinger, ISBN 90 2651 863 3

Deformation analysis of PLPS GRS bridge pier during construction and in service

T. Uchimura, M. Shinoda, M.S.A. Siddiquee & F. Tatsuoka
University of Tokyo, Tokyo, Japan

ABSTRACT: Preloaded and prestressed (PLPS) reinforced soil method aims at substantially increasing the stiffness and decreasing the residual settlement of reinforced soil structures. The first prototype PLPS reinforced soil pier was constructed for a railway bridge in 1996. As a part of a research program to develop a methodology for predicting the time-dependent behaviour of such reinforced soil structures, one of three-component rheology models, named "New Isotach Model", is used to analyze the observed time-dependent (viscous) load-deformation behaviour of the PLPS pier during its preloading procedures.

1 INTRODUCTION

Preloaded and prestressed (PLPS) reinforced soil method aims at substantially increasing its stiffness and decreasing the residual settlement of reinforced soil structures by applying preload and prestress in the vertical direction[1]. Soil structures constructed by this method can be used as important permanent structures to support heavy load without harmful transient and residual deformation. Because soil structures are more flexible than RC structures, they may not be damaged by foundation deformation if it is not excessive. Therefore, a pile foundation, which is required to support RC structures, could become unnecessary. Besides, the construction of reinforced soil structure could be much more cost effective if inexpensive backfill soil is available on site.

The first prototype PLPS geogrid-reinforced soil (GRS) bridge pier was constructed to support a pair of temporary railway girders, each 16.5 m in length, in the summer of 1996 in Fukuoka City, Japan (Figure 1) [2]. This pier has been open to service for more than three years since the summer of 1997. One of three-component rheology models, named "New Isotach Model", is used to analyze the observed load-deformation behaviour of the PLPS pier during its preloading procedures.

2 CONSTRUCTION OF THE PLPS PIER

2.1 *Construction of the pier backfill*

The PLPS geogrid-reinforced soil bridge pier is 6.4 m x 4.4 m in cross-section, and 2.7 m in height. The design dead load by the girder weight and the design live load by train including impact load are 196 kN and 1,280 kN, respectively. Before constructing the pier, an about 9 m-thick very soft clay layer was improved by constructing a set of 0.8 m in-diameter cement-mixed soil columns in-situ. The whole cross-section of a 1 m-thick surface clay layer immediately below the pier was improved by cement-mixing method to form a reaction layer for applying vertical compressive load to the backfill. The lower ends of four steel tie rods with a nominal yield tensile strength of 1,034 kN were anchored into the cement-mixed soil columns for a length of 4 m. A

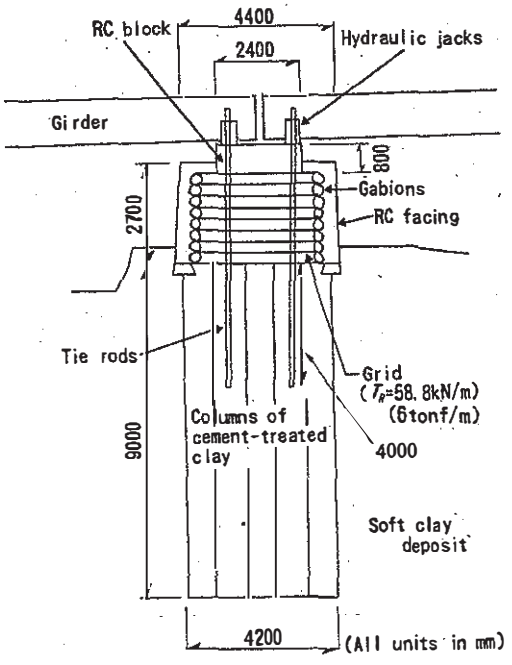

Figure 1. PLPS reinforced soil pier for a railway bridge.

well-graded gravel of crushed sandstone (D_{max} = 30 mm; D_{50} = 0.9 mm; U_c = 16.5; and ϕ=60° at σ'_3 = 50 kPa by triaxial compression tests) was used for the backfill. The backfill was constructed with a help of gravel-filled bags, stacked along the periphery of each gravel layer and wrapped-around with reinforcement. The geogrid reinforcement used was polyvinyl alcohol coated with polyvinyl chloride (PVC). The nominal rupture strength is 73.5 kN/m and the nominal stiffness is 1,050 kN/m at tensile strains less than 1 %. In each of the horizontal two orthogonal axes of the pier, the reinforcement layers were arranged in the same way as usual geosynthetic-reinforced soil retaining walls with a full-height rigid facing having the same height as the pier, constructed under plane strain conditions. The vertical spacing of reinforcement layers was 30 cm. As each cross-section, having one pair of wall faces, of the pier was designed independently, by overlapping the two cross-sections, the actual average vertical spacing of reinforcement layers became 15 cm.

2.2 *Preloading procedures*

A vertical preload of 2,400 kN, equivalent to an average vertical pressure of 200 kPa, was applied to the backfill through the top reaction block by using four hydraulic jacks installed at the top of the tie rods. On the first day, the preload was applied stepwise. During the process of increasing by 200 kN, the load was kept constant for 30 or 60 minutes at each step to allow creep deformation to occur (A in Figure 2). Then constant preload of 2400 kN was applied only during daytime for 2 weeks (B in Figure 2). The backfill was compressed by 8 mm during preloading. Then the load was released to 970 kN (C in Figure 2), and the top ends of the tie rods were fixed to the top RC block to maintain the compressive stress (i.e. prestress) in the backfill. Finally, full-height rigid facings were cast-in-place around the backfill. Since then, nearly constant prestress has worked on the backfill during service (D in Figure 2).

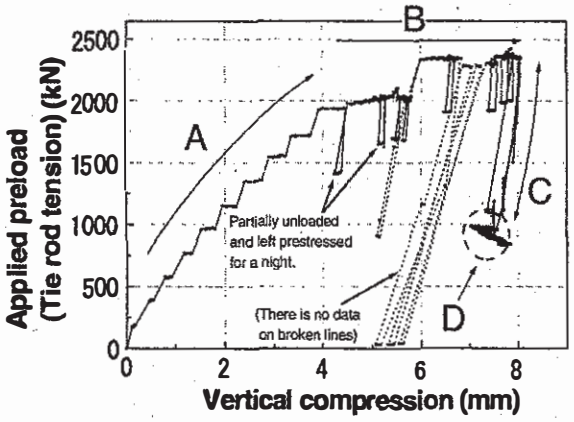

Figure 2. Compression of the pier by preloading.

3 ANALYSIS OF BEHAVIOUR DURING PRELOADING

3.1 *New isotach model*

The long-term deformation of PLPS reinforced soil structures is affected by time-dependent properties of the backfill material and the reinforcement under static and dynamic loading conditions. If the prestress decreases due to creep deformation of the backfill and/or the reinforcement, the stiffness decreases and the transient deformation by traffic load may increase, resulting in large residual deformation. Then, the prestress decreases further, resulting into a phenomenon of vicious spiral. Therefore, it is essential to keep high prestress in the backfill during the life time of structure. As the first step of the study on this topic, it was attempted to analyze the time-dependent deformation of the PLPS reinforced soil pier during preloading (A in Figure 2) based on the new isotach model proposed [3].

The new isotach model is a kind of three component rheology model (Figure 3). According to this model, the total strain increment $d\varepsilon$ consists of elastic strain increment $d\varepsilon^e$ in the component (A) and irreversible strain increment $d\varepsilon^{ir}$ in the components (B) and (C); that is,

$$d\varepsilon = d\varepsilon^e + d\varepsilon^{ir} \tag{1}$$

For the component (A), which is non-linear elastic, the following stress dependency is assumed:

$$\frac{d\sigma}{d\varepsilon^e} = E(\sigma) = E_0\left(\frac{\sigma}{\sigma_0}\right)^m \tag{2}$$

where $d\sigma$ is the stress increment; $d\varepsilon^e$ is the elastic strain increment; σ_0 is the reference stress; $E(\sigma)$ is the Young's modulus as a function of σ; E_0 is equal to $E(\sigma_0)$; and m is a constant. This equation is based on experimental studies (Tatsuoka et. al.[4]).

The total stress σ consists of the time-independent stress σ^f in component (B) and time-dependent stress σ^v in component (C); that is,

$$\sigma = \sigma^f + \sigma^v \tag{3}$$

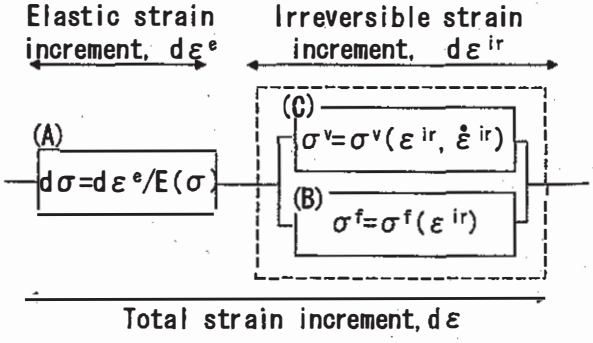

Figure 3. New Isotach model.

where σ^f is a function of irreversible strain ε^{ir} independent of its rate $\dot{\varepsilon}^{ir}$ if the sign of $\dot{\varepsilon}^{ir}$ does not change. If the sign of $\dot{\varepsilon}^{ir}$ changes; i.e. in case of unloading or cyclic loading, the function $\sigma^f = \sigma^f(\varepsilon^{ir})$ changes depending on the loading history. The details of function $\sigma^f(\varepsilon^{ir})$ is unknown at this moment and should be determined based on the results from relevant material tests. σ^v, which controls the time-dependent aspect of the stress-strain behaviour, is a function of ε^{ir} and $\dot{\varepsilon}^{ir}$. Here, the following function is assumed after Tatsuoka et. al.[3].

$$\sigma^v(\varepsilon^{ir}, \dot{\varepsilon}^{ir}) = \sigma^f(\varepsilon^{ir}) \cdot g_v(\dot{\varepsilon}^{ir})$$

$$\text{where, } g_v(\dot{\varepsilon}^{ir}) = \alpha\left[1-\exp\{1-(\frac{\dot{\varepsilon}^{ir}}{\dot{\varepsilon}^{ir}_{ref}}+1)^m\}\right] \qquad (4)$$

where α, m and $\dot{\varepsilon}^{ir}_{ref}$ are the material constants. That is, the compoents (B) and (C) are not independent from each other, as Eq. (4) contains $\sigma^f(\varepsilon^{ir})$. The function $g_v(\dot{\varepsilon}^{ir})$ is a monotonically increasing function, which becomes 0 when $\dot{\varepsilon}^{ir} = 0$ and α when $\dot{\varepsilon}^{ir} = +\infty$. Therefore, we obtain nearly $\sigma = \sigma^f(\varepsilon^{ir})$ under extremely slow loading ($\dot{\varepsilon}^{ir}$ is nearly zero), σ increases as $\dot{\varepsilon}^{ir}$ increases, and nearly $\sigma = (1+\alpha)\sigma^f(\varepsilon^{ir})$ at infinitively high $\dot{\varepsilon}^{ir}$. As the stress-strain relationships are always located between the curves of $\sigma = \sigma^f(\varepsilon^{ir})$ and $\sigma = (1+\alpha)\sigma^f(\varepsilon^{ir})$, they are called the lower and upper bounds, respectively.

According to the new isotach model, the creep behaviour of the materials are explained as follows (Figure 4a). Suppose that the current irreversible strain is ε^{ir} under a given constant stress σ_{creep}. Then the time-independent stress component is given as $\sigma^f = \sigma^f(\varepsilon^{ir})$, and the time-dependent stress component is obtained as $\sigma^v(\varepsilon^{ir}, \dot{\varepsilon}^{ir}) = \sigma_{creep} - \sigma^f(\varepsilon^{ir})$. For the known value of σ_{creep} and the known initial value of ε^{ir}, the initial value of $\dot{\varepsilon}^{ir}$ can be obtained. During the creep stage, as ε^{ir} increases, $\dot{\varepsilon}^{ir}$ decreases according to the decreases in σ^v. After an infinite time period, the stress-strain state reaches the lower bound and stays there.

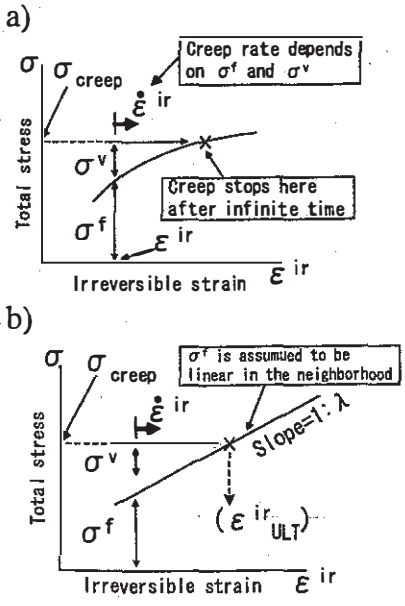

Figure 4. a) Creep deformation according to the new isotach model. b) Assumption with respect to the lower bound for creep analysis.

3.2 *Estimating the parameters for elastic component*

The parameters in Eq. (2), σ_0, E_0 and m, were estimated as follows, based on the results from a triaxial test on a specimen of the backfill gravel used in the PLPS pier (Figure 5a). The specimen had a rectangular prismatic shape with dimensions of 30cm x 30cm x 60cmH. Both the axial and the lateral strains were measured accurately by using LDTs. The material was very densely compacted (γ_t = 2.2 kN/m^3 with a water content of 3.0 %). This density is very likely similar to that of the pier backfill. In order to evaluate the elastic Young's modulus, cyclic axial stresses with a small amplitude (10 kPa) were applied at several stress states during monotonic loading at a constant confining pressure of 49 kPa. Figure. 5b shows the relationships between the obtained Young's modulus and the axial stress in a log-log plot. By linear fitting, the following values were obtained: E_0 = 610 MPa for σ_0 = 100 kPa, and m = 0.63. Using these values, the elastic strain increment $d\varepsilon^e$ was estimated by Eq. (2), and then the irreversible strain $d\varepsilon^{ir}$ was estimated as the difference between total and elastic strains increments (Figure 5a).

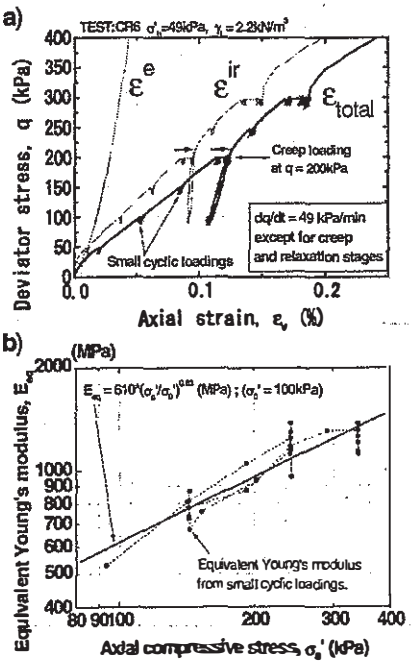

Figure 5. Triaxial test result on the backfill soil of the PL/PS pier:
a) Deviator stress vs. axial strain relation;
b) Young modulus vs. axial stress relation.

3.3 *Estimating the parameters for time-dependent stress component*

The parameters of $g_v(\dot{\varepsilon}^{ir})$ in Eq. (4), α, m and $\dot{\varepsilon}^{ir}_{ref}$ were estimated as follows, also using the results from the triaxial test shown in Figure 5. During monotonic loading, the deviator stress, q = 200 kPa, was kept constant for 1 hour. Figure 6 shows the detailed behaviours. The irreversible strain rate $\dot{\varepsilon}^{ir}$ was obtained by numerically differentiating ε^{ir} with time (Figure 6b and c). Figure 6d show the plot of $\dot{\varepsilon}^{ir}$ against ε^{ir}. In the model, the relationship between $\dot{\varepsilon}^{ir}$ and ε^{ir} is expressed as follows, which is equivalent to the Eq. (4).

$$\dot{\varepsilon}^{ir} = \dot{\varepsilon}^{ir}_{ref}\left[\{1-\ln(1-\frac{x}{\alpha})\}^{1/m}-1\right]$$

$$\text{where } x = g_v(\dot{\varepsilon}^{ir}) = \frac{\sigma_{creep}}{\sigma^f(\varepsilon^{ir})} - 1 \qquad (5)$$

By fitting Eq. (5) to the plot in Figure 6d, the parameters can be determined. However, the function $\sigma^f(\varepsilon^{ir})$ in Eq. (5) is unknown. Therefore, it was assumed that $\sigma^f(\varepsilon^{ir})$ is approximately linear for a limited range of strain for which ε^{ir} changes at each creep loading stage. Then x in Eq. (5) can be expressed as follows (Figure 4b):

$$x = g_v(\dot{\varepsilon}^{ir}) = \frac{\sigma_{creep}}{\sigma^f(\varepsilon^{ir})} - 1 = \frac{\lambda\bullet(\varepsilon^{ir}_{ULT} - \varepsilon^{ir})}{\sigma_{creep} - \lambda\bullet(\varepsilon^{ir}_{ULT} - \varepsilon^{ir})} \qquad (6)$$

where ε^{ir}_{ULT} is the irreversible strain when the stress-strain state is on the lower bound, and λ is the slope of the lower bound that is linearly fitted for a stress rate around the current stress level. This assumption is acceptable because, for usual geomaterials, the stress-strain relationships before failure is smooth without sudden changes in its tangent modulus.

By fitting Eqs. (5) and (6) to the data plotted in Figure 6d, the values of the five parameters, α, m, $\dot{\varepsilon}^{ir}_{ref}$, λ and ε^{ir}_{ULT}, were obtained. The values of α, m and $\dot{\varepsilon}^{ir}_{ref}$ are considered to be specific to the material, while λ and ε^{ir}_{ULT} change at each creep stage. It was shown that several different combinations of parameters gives similarly good fitting to the same plot (Table 1). The relations using the parameter combinations with, for example, α=0.09004 and α=10 are also shown in Figure 6d. It is possible that there exist a set of parameter values which give similarly good fitting for each values of α. One of the reasons is that the range of ε^{ir} encountered in the data shown in Figure 6d is much more narrow than the full range dealt with by Eqs. (5) and (6) The other reason may be that there is a large redundancy among the five parameters. It is also possible that other models are more relevant to be present case. Dan et al. (2001)[5] used the so-called general TESRA model to simulate triaxial compression test reults of a dense well-graded gravel. This point should be studied more. Herein, the combination with α=15 was used because for a reason mentioned later.

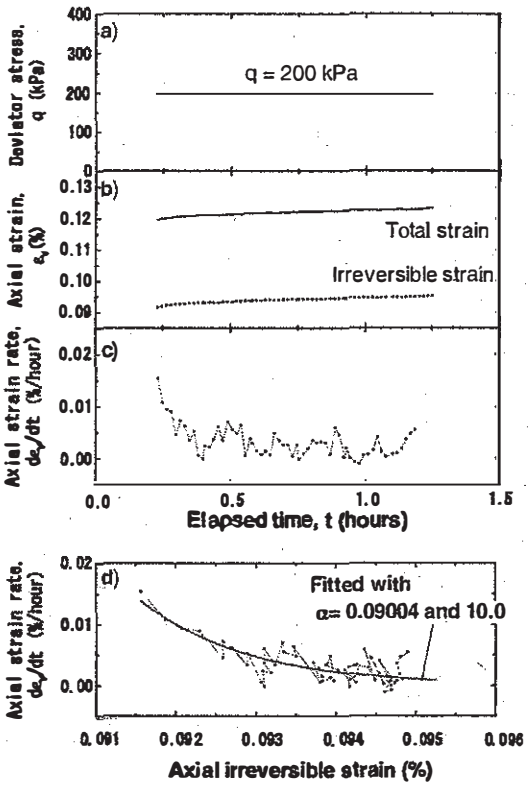

Figure 6. Details of triaxial creep test on the backfill soil.
a) Deviator stress vs. time relation.
b) Total and irreversible strain vs. time relation.
c) Rate of irreversible strain vs. time relation.
d) Irreversible strain vs. its rate relation.

Table 1. Obtained parameters of time-dependent irreversible component

α	m	$\dot{\varepsilon}^{ir}_{ref}$	λ	ε^{ir}_{ULT}
0.09004	0.0137	0.000224188	226.934	0.09716
0.5	0.00589	0.000090750	518.0	0.09861
1	0.00414	0.000072450	726.5	0.09889
5	0.00194	0.000029659	1623.6	0.10022
10	0.0015	0.000018106	2351.8	0.10118
15	0.0013	0.000015034	2898.8	0.10168

3.4 *Estimating the parameters for time-independent stress component (lower bound)*

The lower bound function for the PLPS pier during preloading was estimated as follows. The elastic and irreversible deformations of the pier during the first day of preloading were estimated by using the parameters obtained above as shown in Figure 7. The deformation is expressed in the strain averaged for a backfill height of 2.4 m, and the load is expressed in the average stress estimated at the mid-height of the backfill (cross-sectional area is 22.04 m^2). In the lower part of Figure 7, the relationships between the irreversible strain ε^{ir} and its rate $\dot{\varepsilon}^{ir}$, obtained in the same way as shown in Figure 6d, are shown. Eqs. (5) and (6) are fitted reasonably well to the relationship between ε^{ir} and $\dot{\varepsilon}^{ir}$ for the respective creep stage. Here, fixed parameters α=15, m=0.0013 and $\dot{\varepsilon}^{ir}_{ref}$=0.000015034, from Table 1, were used, while λ and ε^{ir}_{ULT} were changed to optimize the fitting. As mentioned before, ε^{ir}_{ULT} presents the ultimate value of ε^{ir} when the stress-strain state reaches the lower bound after an infinitively long period of creep. These ultimate points are denoted by the symbol "×" in Figure 7. The following lower bound function was obtained by fitting to these ultimate points.

$$\sigma^f(\varepsilon^{ir}) = (34.84 + 644.1\,\varepsilon^{ir})/(1+2.241\,\varepsilon^{ir}) \qquad (7)$$

Figure 8 shows the ultimate points at the respective creep stage obtained by using the same method for different values of parameter α, 0.09004, 10 and 15. The arrows represent the instantaneous tangent slope of the lower bound, λ, obtained at each point. With α = 15, the arrows are directed to the ultimate point at the immediately preceding creep stage, validating the value of α = 15. With α = 10, nearly the same results are obtained. On the other hand, wiht α = 0.09004, the directions of the arrows are nearly horizontal, showing that the value of α = 0.09004 is not appropriate. The method described above may be one of the methods to choose the most appropriate parameters from possible values as listed in Table 1.

Following the preloading in the first day, the tie rods were fixed to the top reaction block by using nuts for a period of one night with some compressive stress remaining in the backfill (A in Figure 8). For this period, the backfill expanded in the vertical direction due to creep recovery. According to the new isotach model, creep recovery can take place only when the stress-strain state is below the lower bound. Thus the lower bound should be located above A in Figure 8. This may be another information to determine the parameters.

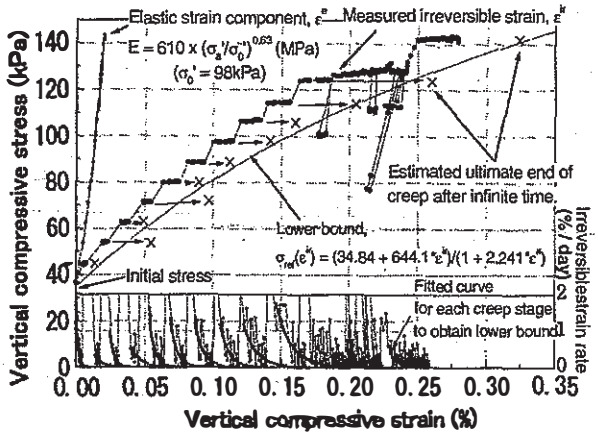

Figure 7. Lower bound of the PL/PS pier during preloading obtained by New Isotach model.

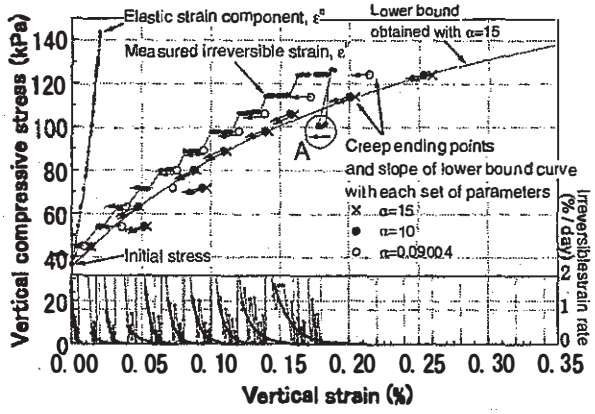

Figure 8. Lower bounds obtained by using different parameters.

3.5 *Simulation of the behaivour during preloading*

Using the parameters obtained above, the behaviour of the pier backfill during preloading was simulated (Figure 9). The recorded tme history of the average stress was given to simulate the irreversible strain. The amount of the simulated creep deformation during each creep stage agrees very well with the respective measured value. However, the global irreversible strain is over-estimated. The stress-strain relationships when the load was increasing rapidly are noticeably different between the measurement and the simulation. It is likely that this difference is due at least partly to that the full detailed measured relationships could not be obtained due to a too long sampling interval (2 minutes). Especially in estimating the parameters for the time-independent stress component (the lower bound), the data used for curve fitting for each creep loading stage are too few in number and too much fluctuating (Figure 7). This may have caused a large error in the estimated lower bound. Figure 10 shows the simulation obtained by using a modified lower bound (the value of $\sigma^f(\varepsilon^{ir})$ has been multiplied by 1.2) with the same values for

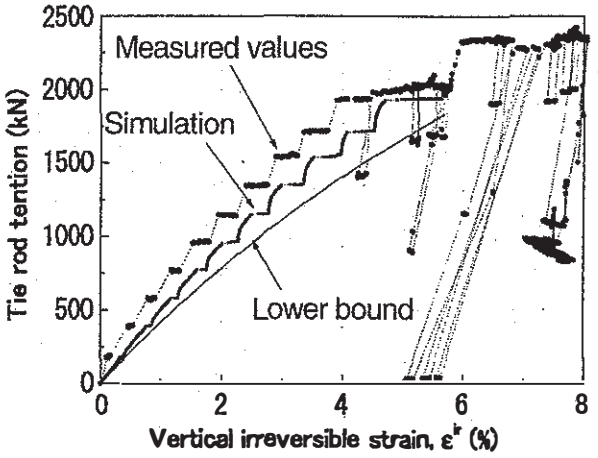

Figure 9. Lower bound of the PL/PS pier during preloading obtained by new isotach model.

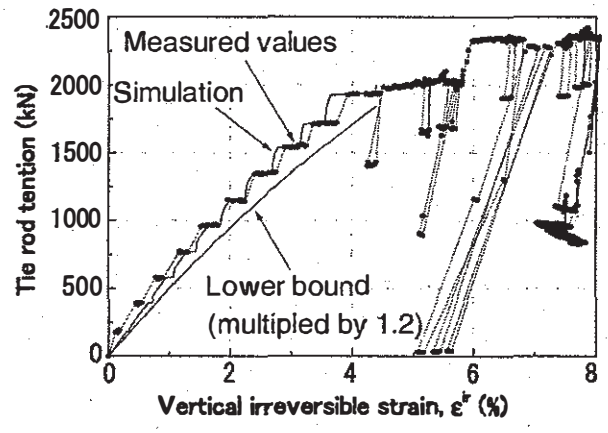

Figure 10. Lower bounds obtained by using different parameters.

the other model parameters as the case of Figure 9. The simulation and measured values agree with each other to a better than Figure 9, but such a procedure of determining parameters as above is logically inconsistent. Further study on this method based on more accurate data from element tests on the materials are necessary.

4 CONCLUSIONS

A method of numerical analysis based on the new isotach model of the time-dependent behaviour of the pier backfill was proposed. However, this simulation method is not sufficient in the following important factors, which should be studied in the next step.

1) The new isotach model should be fully validated based on results from a comprehensive series of accurate tests of the backfill and reinforcement materials.
2) The model is one-dimensional in the sense that only the relationship between one stress component (vertical stress) and the one strain component (vertical strain) is simulated, ignoring the horizontal stress and strain relationship. The latter is essential to evaluate the time-dependent behaviour of the reinforcement placed in the horizontal direction and the interaction between the backfill and the reinforcement.
3) The simulation by the new isotach model of the observed time-dependent behaviour during unloading, which is essential for the proposed PLPS construction method, should be attempted.
4) A model that can simulate and predict the transient and residual deformation of the backfill by traffic load, which applies a great number of small cyclic load to the backfill for a very long duration, should be developed.

REFERENCES

Tatsuoka,F., Uchimura,T., and Tateyama, M. 1997. Preloaded and prestressed reinforced soil, *Soils and Foundations*, 37(3): 79-94

Uchimura,T., Tatsuoka,F., Tateyama,M., Koga,T. 1998. Preloaded-Prestressed Geogrid reinforced Soil Bridge Pier, *Proc. 6th Int. Conf. on Geosynthetics, Atlanta*, Vol.2: 565-572.

Tatsuoka,F., Uchimura,T., Hayano,K., Di Benedetto,H., Koseki,J. and Siddiquee,M.S.A. 1999. Time-dependent deformation characteristics of stiff geomaterials in engineering practice, the Theme Lecture, *Proc. of the Second International Conference on Pre-failure Deformation Characteristics of Geomaterials, Torino, Balkema (Jamiolkowski et al., eds.)*, Vol. 2 (to appear).

Tatsuoka,F., Jardine,R.J., Lo Presti,D., Di Benedetto,H. and Kodaka,T. 1999. Characterising the Pre-Failure Deformation Properties of Geomaterials, *Theme Lecture for the Plenary Session No.1, XIVIC on SMFE, Hamburg*, Vol. 4: 2129-2164.

AnhDan, LQ., Koseki,J. and Tatsuoka,F. 2001. Viscous deformation in triaxtial compression of a dense well graded gravel and its model simulation, submitted to Summary Book of TC29, ISSMGE.